Microvessel Density: Correlation with ^{18}F-FDG Uptake and Prognostic Impact in Lung Adenocarcinomas

JianFei Guo, MD[1,2]; Kotaro Higashi, MD[1]; Yoshimichi Ueda, MD[3]; Manabu Oguchi, MD[1]; Tsutomu Takegami, MD[4]; Hirohisa Toga, MD[5]; Tsutomu Sakuma, MD[6]; Hajime Yokota, MD[1]; Shogo Katsuda, MD[3]; Hisao Tonami, MD[1]; and Itaru Yamamoto, MD[1]

[1]Department of Radiology, Kanazawa Medical University, Ishikawa, Japan; [2]Department of Radiology, First Affiliated Hospital, China Medical University, Shenyang, People's Republic of China; [3]Department of Pathology, Kanazawa Medical University, Ishikawa, Japan; [4]Department of Medical Research Institute, Kanazawa Medical University, Ishikawa, Japan; [5]Division of Respiratory Disease, Department of Internal Medicine, Kanazawa Medical University, Ishikawa, Japan; and [6]Department of Thoracic Surgery, Kanazawa Medical University, Ishikawa, Japan

Although researched for many years, the prognostic value of tumor angiogenesis reflected by microvessel density (MVD) is still controversial, and there have been no previous reports regarding the correlation with ^{18}F-FDG uptake in lung adenocarcinomas. Therefore, in the present study, we investigated the correlation between MVD determined with different endothelial cell antibodies and ^{18}F-FDG uptake and compared the prognostic impact of those factors in lung adenocarcinomas. **Methods:** Forty-four patients with 45 lung adenocarcinomas underwent ^{18}F-FDG PET before surgery. Consecutive paraffin-embedded sections obtained from each resected tumor were immunostained for CD31 (a panendothelial cell marker), CD105 (a proliferation-related endothelial cell marker), and CD34/α-SMA (for double labeling of endothelial cells and mural cells). Four high-power fields in the area with the highest MVD were selected for analysis. Computer-assisted image analysis was used to assess MVD. **Results:** MVD staining results for panendothelial cell markers can be classified into 3 microvessel patterns: diffuse, alveolar, and mixed. The highly ordered alveolar pattern is believed to represent preexisting alveolar vessels trapped in lung adenocarcinomas and may have no significant meaning for the aggressiveness of tumors. Preexisting alveolar cells also do not contribute to ^{18}F-FDG uptake. CD105 staining of MVD (CD105-MVD) showed a significantly positive correlation with ^{18}F-FDG uptake ($P < 0.0001$), whereas CD31 staining of MVD (CD31-MVD) showed a marginally negative correlation with it ($P = 0.057$). Although CD105-MVD correlated negatively with prognosis, patients with low CD105-MVD, compared with those with high or moderate CD105-MVD, had a much better prognosis in both disease-free and overall survival analyses ($P = 0.017$ and $P = 0.013$, respectively). Patients with low CD31-MVD had the worst prognosis ($P = 0.032$ for disease-free survival analysis and $P = 0.179$ for overall survival analysis). **Conclusion:** There is no positive correlation between ^{18}F-FDG uptake and MVD determined with panendothelial cell markers (CD31 and CD34); in contrast, there is a marginally negative correlation between them. MVD determined with CD105, which is a proliferation-related endothelial cell marker, reflects active angiogenesis, correlates positively with ^{18}F-FDG uptake, and is a better indicator of prognosis in lung adenocarcinomas.

Key Words: PET; ^{18}F-FDG; lung cancer; microvessel density; prognosis

J Nucl Med 2006; 47:419–425

Lung cancer is the leading reason for cancer-related deaths in Japan and most Western countries. Surgery is the main method of therapy and also can be combined with radiotherapy and chemotherapy. However, the mortality of lung cancer is still very high; the 5-y survival expectation is only 70%–80%, even in the very early stages (*1,2*). Adenocarcinoma is the most common histologic type of lung cancer and accounts, to a great extent, for the increasing incidence of lung cancer in recent years (*3*). The established prognostic criteria for patients with non–small cell lung carcinoma (NSCLC), such as pathologic stage, can serve as a good indicator of a patient's outcome; however, this staging system does not determine accurately an individual patient's prognosis. Therefore, there is an urgent need to identify and validate new molecular markers and imaging techniques to better identify patients at risk for recurrent disease and metastatic disease, so that patients who might benefit from adjuvant therapy after surgery can be selected.

Tumor angiogenesis is an essential requirement for the development, progression, and metastasis of malignant tumors (*4*). Immunohistochemical staining measurements of angiogenesis with antibodies to factor VIII, CD31, CD34, or CD105 can be used to determine microvessel density (MVD), an important prognostic factor that is independent of other known prognostic variables in several

Received Aug. 16, 2005; revision accepted Nov. 30, 2005.

For correspondence or reprints contact: Kotaro Higashi, MD, Department of Radiology, Kanazawa Medical University, 1-1, Daigaku, Uchinada, Kahoku-gun, Ishikawa 920-0293, Japan.

E-mail: h550208@kanazawa-med.ac.jp

cancer types (*5*), including lung cancer (*6–12*). However, whereas some reports have found that MVD is an important prognostic factor in lung cancer (*6,7,10,12*), some reports have failed to do so (*8,9,11*). Therefore, although MVD estimation has promising prognostic prospects, a consensus as to whether MVD is a prognostic marker in lung cancer has yet to be reached.

^{18}F-FDG PET has been applied in many kinds of tumors and is regarded as a good imaging technique for predicting prognosis in some tumors (*13,14*), especially lung cancer (*15–19*). In previous studies, it was demonstrated that ^{18}F-FDG uptake is a significant prognostic factor in patients with NSCLC or adenocarcinoma (*16,19*)—and is even better than pathologic stage (*16*). Furthermore, some studies showed that there is a significant correlation between ^{18}F-FDG uptake and blood flow in breast cancer (*20*). However, although tumor angiogenesis showed a correlation with blood flow, the 2 factors are still quite different from each other. To date, there has been no report regarding the correlation between MVD and ^{18}F-FDG uptake in lung adenocarcinoma. Therefore, in the present study, we investigated not only whether tumor angiogenesis reflected by MVD determined with CD31 or CD105 is a good prognostic factor but also whether there is any correlation between MVD and ^{18}F-FDG uptake in patients with lung adenocarcinoma.

MATERIALS AND METHODS

Patients

Forty-four patients (20 men and 24 women; age range, 47–82 y; mean age, 65 y) with 45 lung adenocarcinomas were included in this study. Twelve patients had bronchioloalveolar carcinoma (BAC), 12 had well-differentiated adenocarcinoma, 14 had moderately differentiated adenocarcinoma, 5 had poorly differentiated adenocarcinoma, and 1 had 2 types of cancer (moderately differentiated adenocarcinoma and poorly differentiated adenocarcinoma). All patients underwent a thoracotomy within 4 wk after their ^{18}F-FDG PET study. No patient had received neoadjuvant chemotherapy or radiotherapy before surgery. Final diagnoses were established histologically (via the thoracotomy) in all patients, and the pathologic stage of each tumor was recorded with the TNM staging system. The sizes of the tumors were determined from the resected specimens and ranged in diameter from 1.2 to 5.5 cm. None of the patients had insulin-dependent diabetes, and the serum glucose levels in all patients just before ^{18}F-FDG injection were less than 120 mg/dL. Informed consent was obtained from all patients participating in this study.

^{18}F-FDG PET Imaging

^{18}F-FDG PET was performed by use of a PET camera (Headtome IV; Shimadzu) with a 10-cm axial field of view. The Headtome IV has 4 detector rings with 768 bismuth germanate crystals per ring. It uses direct and cross-plane coincidence detection to generate 14 slices per bed position. For the thorax, 2 bed positions (28 slices at 6.5-mm intervals) were obtained. Reconstruction in a 128 × 128 matrix with a Hann filter (0.5 cutoff) yielded 5-mm intrinsic resolution at the center. Transmission scans were obtained in all subjects before ^{18}F-FDG administration for attenuation correction with a ^{68}Ge ring source. x-Ray fluoroscopy was used to ascertain the location of the pulmonary nodule, and marks were made on the skin to aid in positioning the patient for the transmission scan. A transmission scan was acquired for 10–20 min in each bed position, depending on the specific radioactivity of the ring sources at the time of the study, for at least 2 million counts per slice. During the transmission scan, marks were made on the patient's skin to aid in repositioning for the emission scan. However, because of the limitation of the available equipment, we could not perform respiratory gating to avoid respiratory motion, which may affect the standardized uptake value (SUV) to some degree. Blood (1 mL) was drawn for baseline blood glucose estimation, and the data were recorded. Immediately after the transmission scan, ^{18}F-FDG was administered intravenously. The average injected dose of ^{18}F-FDG was 185 MBq. After a 40-min uptake period, the patient was repositioned in the scanner. An emission scan was acquired for 10 min in each bed position; the process took a total of 20 min.

For semiquantitative analysis of ^{18}F-FDG uptake, regions of interest (ROIs) were manually defined on the transaxial tomograms that showed the highest uptake to be in the middle of the tumor. The ROIs placed on the lesions encompassed all pixels within lesions that had uptake values of greater than 90% the maximum uptake in that slice, and the average count rate in each ROI was calculated. In patients in whom no nodules were detectable by PET, the ROIs were extrapolated from chest CT scans. After correction for radioactive decay, we analyzed the ROIs by computing the SUVs as follows: PET counts per pixel per second times calibration factor per injected dose (MBq) per kilogram of body weight, where the calibration factor was (MBq/mL)/(counts/pixel/s).

Immunohistochemical Analysis

Immunohistochemical Analysis with a Panendothelial Cell Marker. Monoclonal antibody (mAb) JC70 (Dako), recognizing panendothelial cell antigen CD31 (platelet/endothelial cell adhesion molecule), was used for microvessel staining of 5-μm paraffin-embedded sections. Sections were dewaxed, rehydrated, and microwaved (3 times for 4 min each time) for antigen retrieval. Endogenous peroxidase activity was blocked by incubation in 0.3% hydrogen peroxide in methanol. Nonspecific protein binding was inhibited by treatment with 10% normal serum for 10 min at 37°C. The specimens then were incubated with mAb JC70 overnight at 4°C. The slides were preincubated and rinsed in phosphate-buffered saline and then treated with the biotinylated secondary antibody and peroxidase-conjugated streptavidin. The final reaction product was revealed by exposure to 0.03% diaminobenzidine, and the nuclei were counterstained with Mayer hematoxylin. As a negative control, appropriately diluted nonimmune sera were applied instead of the primary antibody.

Immunohistochemical Analysis with a Proliferation-Related Endothelial Cell Marker. CD105 was stained with mAb SN6 h (1:100; Dako) (*21*) by use of a sensitive immunohistochemical staining system (CSA System; Dako). All of the procedures were performed in accordance with the manufacturer's protocol. Sections were incubated with the anti-CD105 mAb diluted 1:100 for 1 h at room temperature. Normal mouse IgG was used instead of the primary antibody as a negative control.

Double-Labeling Immunohistochemical Technique for CD34 and α-SMA. A double-labeling immunohistochemical technique with a specific double-labeling kit (Envision+ System; Dako) was

used to simultaneously stain endothelial cells (CD34) and mural cells (α-SMA) (*22*) to quantitatively assess the pericyte coverage of microvessels. Peroxidase activity was blocked in deparaffinized and rehydrated tissue sections, and the sections were trypsinized, incubated with blocking serum, and then doubly stained for CD34 to label endothelial cells and for α-SMA to detect pericytes and smooth muscle cell expression. For CD34 staining, sections were incubated with a mouse mAb (clone BI-3C5, 1:50 dilution; Zymed) overnight at 4°C. A biotinylated secondary antibody, streptavidin–alkaline phosphatase complex, and diaminobenzidine as a substrate were used to visualize binding of the CD34 antibody. For subsequent staining of α-SMA, sections were incubated with a mouse anti–human α-SMA mAb (clone 1A4, 1:50 dilution; Sigma) for 2 h at room temperature. The color was developed by 20 min of incubation with new fuchsin solution.

Assessment of MVD

Assessment of MVD was performed by computer-assisted image analysis as suggested previously but with some modifications (*23,24*). Vessels with a clearly defined lumen or well-defined linear vessel shape but not single endothelial cells were considered for microvessel assessment. The areas with the highest vascularization were scanned and chosen at low power (×100), and 4 chosen ×200 fields with the highest vascularization were recorded with a digital camera. The captured images were 24 bit and had a resolution of 2,272 × 1,704 pixels. Adobe Photoshop (version 6.0; Adobe Systems Inc.) was used to outline microvessels and convert the images into binary, black-and-white images; the converted images were imported into the image analysis package NIH image 1.62 (http://rsb.info.nih.gov/nih-image/) to calculate the percentage of stained microvessel area corresponding to the total section area. The average MVDs of the 4 selected areas were grouped into 3 grade categories. For CD31 staining of MVD (CD31-MVD), the categories were as follows: low, 0%–4%; moderate, 4%–8%; and high, >8%. For CD105 staining of MVD (CD105-MVD), the categories were as follows: low, 0%–0.8%; moderate, 0.8%–1.6%; and high, >1.6%.

Statistical Methods

All data are reported as the mean ± 1 SD. All statistical analyses were performed with SPSS for Windows (version 12.0; SPSS Inc.). The χ-square test was used to compare the distributions of values across categoric variables. Differences between continuous variables and dichotomous variables were tested by 1-way ANOVA. Overall and disease-free survival probabilities were calculated with the Kaplan–Meier life table method. Differences between survival probabilities were analyzed by the log-rank test. Probability values of less than 0.05 were considered statistically significant.

RESULTS

Vascular Architecture in Lung Adenocarcinomas

On the basis of the immunohistochemical staining results obtained with antibody against CD31, the vascular architecture in lung adenocarcinomas usually can be classified into 3 kinds of patterns: diffuse, alveolar, and mixed. The diffuse pattern is an angiogenic pattern. Normal lung architecture is replaced diffusely. Vessels and stroma are scattered randomly throughout the tumor (Fig. 1A). The alveolar pattern is a nonangiogenic pattern. Tumor cells fill up the alveoli, exploiting the existing alveolar vessels instead of destroying them (Fig. 1B). The mixed pattern consists of both diffuse and alveolar patterns.

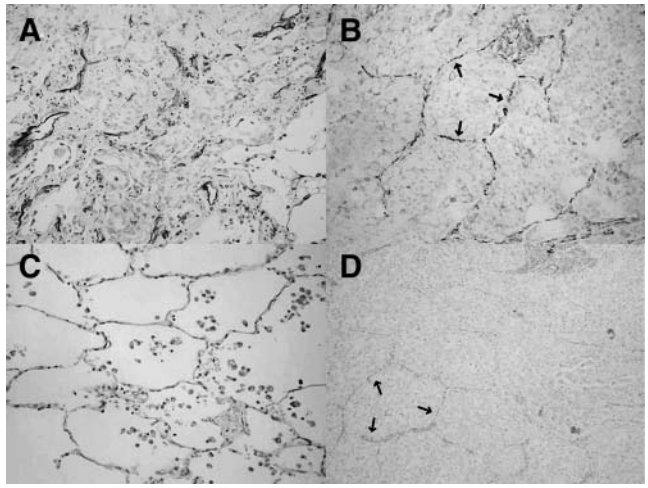

FIGURE 1. (A) Adenocarcinoma with diffuse pattern stained by mAb to CD31. Normal structure was destroyed, and vessels were randomly and diffusely distributed throughout tumor. (B) Adenocarcinoma with alveolar pattern stained by mAb to CD31. Vessels (arrows) in alveolar pattern area were in original distribution; tumor cells filled up alveoli instead of destroying them. (C) Normal alveoli. (D) Consecutive section of same tumor as in B stained by mAb to CD105. Trapped vessels showed negative staining (arrows).

Comparison Between CD34/α-SMA and CD105

For serial sections of lung adenocarcinomas, we compared immunohistochemical staining by mAbs against CD34 (Fig. 2A) and CD105 (Fig. 2B). For CD34 staining, we used a double-labeling technique, staining CD34-positive vessels and vascular pericytes simultaneously. Because the mAb against α-SMA is targeted specifically to pericytes and smooth muscle cells (*22*), vessels with α-SMA expression are mature vessels, and vessels without α-SMA expression are newly formed immature vessels. The total vessel number is usually much higher with CD34 staining and lower with CD105 staining in the same sample; however, as shown in Figure 2, CD34 staining was seen for both mature and immature vessels, whereas CD105 staining was seen mainly for immature vessels. Staining by a mAb against CD31 showed results similar to those for CD34; both mature and immature vessels were stained in the tumors.

Correlation Between MVD and Clinicopathologic Parameters

Table 1 shows the results of a comparison of CD31-MVD and CD105-MVD with clinicopathologic parameters. CD31-MVD showed a correlation with patient age (P = 0.042), sex (P = 0.049), and histologic findings (P = 0.017), whereas CD105-MVD showed a correlation with stage (P = 0.004), tumor size (P = 0.031), and histologic findings (P = 0.007). Our data showed that solitary BAC, a

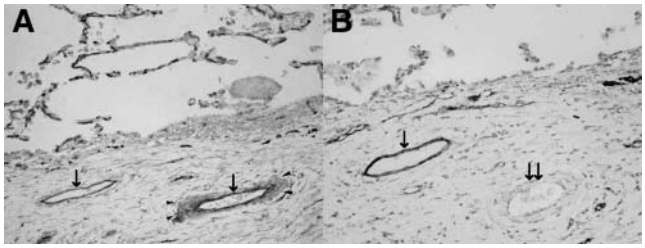

FIGURE 2. Comparison between CD34/α-SMA double labeling and CD105 in serial sections. (A) Double labeling of CD34 (arrow) and α-SMA (arrowheads). Left vessel was immature vessel showing staining only with CD34. Right vessel was mature vessel showing staining with both CD34 and α-SMA. (B) CD105 staining. Only left, immature vessel was positive for CD105 (arrow). Right, mature vessel was negative for CD105 (double arrows).

subcategory of lung adenocarcinoma with a good prognosis and an MVD that is different from those of other types of adenocarcinoma, had moderate or high CD31-MVD and CD34-MVD but low CD105-MVD.

Correlation Between MVD and ^{18}F-FDG Uptake

Figure 3 shows the correlation of CD31-MVD and CD105-MVD with ^{18}F-FDG uptake. ^{18}F-FDG uptake showed a marginally negative correlation with CD31-MVD ($P = 0.057$), whereas it showed a significantly positive correlation with CD105-MVD ($P < 0.0001$).

Correlation Between MVD and Postoperative Prognosis

Using the Kaplan–Meier method, we analyzed the prognostic impact of CD31-MVD and CD105-MVD in lung adenocarcinomas (Fig. 4). Patients with moderate CD31-MVD had the best disease-free and overall survival probabilities, and patients with low CD31-MVD had the worst prognosis ($P = 0.032$ for disease-free survival analysis and $P = 0.179$ for overall analysis). CD105-MVD correlated negatively with prognosis; patients with low CD105-MVD had the best disease-free and overall survival probabilities ($P = 0.017$ and $P = 0.013$, respectively).

Figures 5 and 6 show 2 representative cases in this study.

DISCUSSION

The present study demonstrated that there is no positive correlation between ^{18}F-FDG uptake and MVD determined with panendothelial cell markers (CD31 and CD34); in contrast, there is a marginally negative correlation between them. Furthermore, MVD determined with CD105, which is a proliferation-related endothelial cell marker, reflects active angiogenesis, correlates positively with ^{18}F-FDG uptake, and is a better indicator of prognosis in lung adenocarcinomas.

Angiogenesis is essential for neoplastic proliferation, progression, invasion, and metastasis because solid tumors cannot grow beyond 1–2 mm in diameter without angiogenesis (*25*). MVD is assumed to reflect the intensity of tumor angiogenesis; indeed, it has been established as a good indicator of prognosis in several cancer types (*5*). However, conflicting results on the prognostic impact of MVD in lung cancer make it difficult to determine the prognostic importance of tumor angiogenesis in lung cancer (*6–12*). Variations in survival results among studies could be explained by the heterogeneity in methodologies used to stain and count microvessels in tumors in addition to variations in patient populations. Differences in reactivity between anti–endothelial cell antibodies used to highlight intratumoral microvessels represent a major bias that should be considered. Although antibodies to CD31 and

TABLE 1
Relationship of Clinicopathologic Parameters to MVD

Parameter	CD31-MVD*			*P*	CD105-MVD*			*P*
	Low	Moderate	High		Low	Moderate	High	
Age				0.042				0.254
≤65	10	9	3		11	5	6	
>65	4	9	10		6	8	9	
Sex				0.049				0.376
Male	10	5	6		6	6	9	
Female	4	13	7		11	7	6	
Stage				0.223				0.004
I	11	13	7		16	9	6	
II, III	3	2	5		0	3	7	
Size				0.234				0.031
≤3 cm	8	14	11		16	9	8	
>3 cm	6	4	2		1	4	7	
Histologic findings				0.017				0.007
BAC	0	8	4		9	2	1	
Non-BAC	14	10	9		8	11	14	

*Data are reported as number of tumors.
Non-BAC = well-differentiated adenocarcinoma, moderately differentiated adenocarcinoma, and poorly differentiated adenocarcinoma.

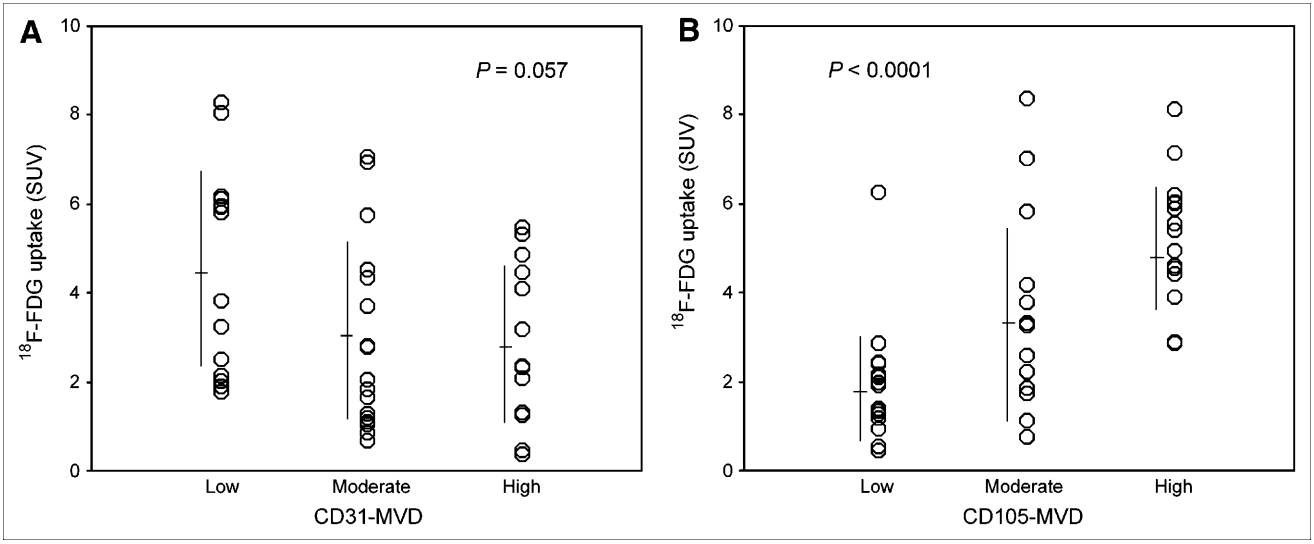

FIGURE 3. (A) CD31-MVD showed negative correlation with ^{18}F-FDG uptake ($P = 0.057$). (B) CD105-MVD showed significantly positive correlation with ^{18}F-FDG uptake ($P < 0.0001$).

CD34 are recommended as standard antibodies for assessing MVD in solid tumors (*26,27*), the variations among studies with these antibodies imply their limitations in lung cancer.

Endothelium in healthy adults is considered quiescent because the turnover of endothelial cells is very low (*28*). However, endothelial cells of tumor-associated neovasculature proliferate 20–2,000 times more rapidly than do endothelial cells of normal tissues (*29*). CD105 (endoglin) is a homodimeric cell membrane glycoprotein expressed on endothelial cells and is thought to be a proliferation-associated marker of endothelial cells (*30,31*). In fact, a correlation has been found between levels of CD105 expression and markers of cell proliferation (i.e., cyclin A and Ki-67) in tumor endothelia (*32*), and some studies have indicated that a greater intensity of staining for CD105 is detectable in blood vessel endothelia within neoplastic tissues than in those within normal tissues (*31,33*). Consistent with these findings, CD105 has been shown to represent an ideal marker for quantifying tumor angiogenesis and to be an independent indicator of prognosis in some tumors (*34,35*), including lung cancer (*21*).

In the present study, by comparing staining results for CD105 and CD34/α-SMA in serial sections of lung adenocarcinomas, we found that CD105 was expressed specifically in immature vessels but not in mature vessels. In areas with an alveolar pattern, we could see clearly the difference between CD31 expression and CD105 expression. The trapped vessels were in the same distribution as in normal alveoli; however, these kinds of vessels were CD31 positive but CD105 negative. Taken together, these findings indicated the following. First, there may be a different mechanism of tumor angiogenesis in lung adenocarcinomas—involving tumor cells filling the alveolar spaces and entrapping, but not destroying, the alveolar septa and co-opting the preexisting blood vessels. Second, because of the presence of the alveolar pattern, comparing the proliferation-related endothelial cell marker CD105 with panendothelial cell markers, such as factor VIII, CD31, and CD34, may not reflect exactly the tumor-associated neovasculature; this may be one of the explanations for the conflicting results regarding MVD studies in lung cancer. Third, although there is a marginally significant correlation between CD31-MVD and prognosis, CD105-MVD has a much more significant prognostic impact than does CD31-MVD; therefore, CD105-MVD is a much better indicator of prognosis in lung adenocarcinomas.

Furthermore, we also found that BAC usually has moderate or high CD31-MVD and CD34-MVD but low CD105-MVD. BAC, as a subcategory of lung adenocarcinoma, has a fairly good prognosis for surgically treated patients. The key pathologic feature of BAC is preservation of the underlying architecture of the lung, with cylindric tumor cells growing on the walls of preexisting alveoli. Therefore, because CD31 and CD34 staining was seen for both mature and immature vessels, it is reasonable to assume that the moderate or high CD31-MVD and CD34-MVD involved mainly preexisting vessels; serial sections stained with CD105 further proved that those vessels were negative for CD105. Although the pathophysiologic impact of preexisting vessels for tumor progression is still unclear, it seems that these kinds of vessels make no contribution to ^{18}F-FDG uptake in lung adenocarcinomas, because most solitary BACs are almost negative in ^{18}F-FDG PET (*36*), even though these BACs have moderate or high CD31-MVD and CD34-MVD.

Regarding the correlation between ^{18}F-FDG uptake and MVD in NSCLC, only 1 previous study mentioned a positive correlation between ^{18}F-FDG uptake and CD34-MVD (*37*). The present study is the first research concentrating

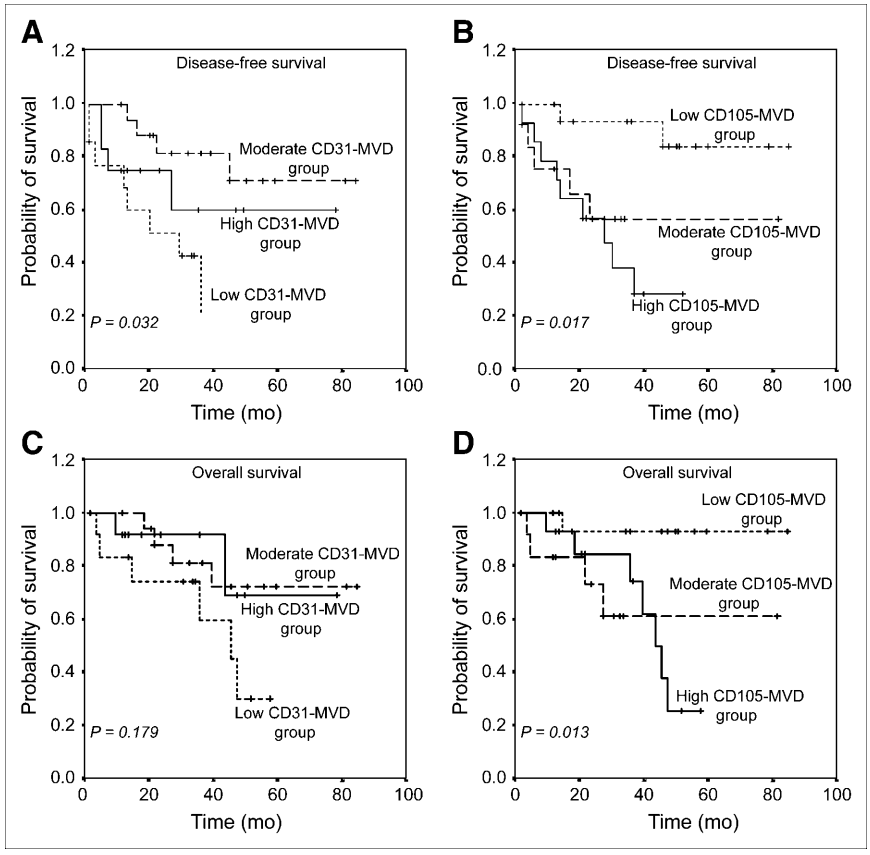

FIGURE 4. Kaplan–Meier survival curves based on MVDs in lung adenocarcinomas. Patients with low CD31-MVD had worst disease-free and overall survival probabilities (A and C), whereas patients with low CD105-MVD had best disease-free and overall survival probabilities (B and D).

on the correlation in lung adenocarcinomas. In contrast to that previous study, our findings suggested that ^{18}F-FDG uptake shows a marginally negative correlation with CD31-MVD but a significantly positive correlation with CD105-MVD. However, the underlying mechanism of this difference is still unclear, and further study is warranted. Although the prognostic impact of MVD in NSCLC is complicated and further study is needed, a new treatment for malignant tumors (antiangiogenic therapy) recently provided new hope for cancer therapy (*38*). Therefore, there is

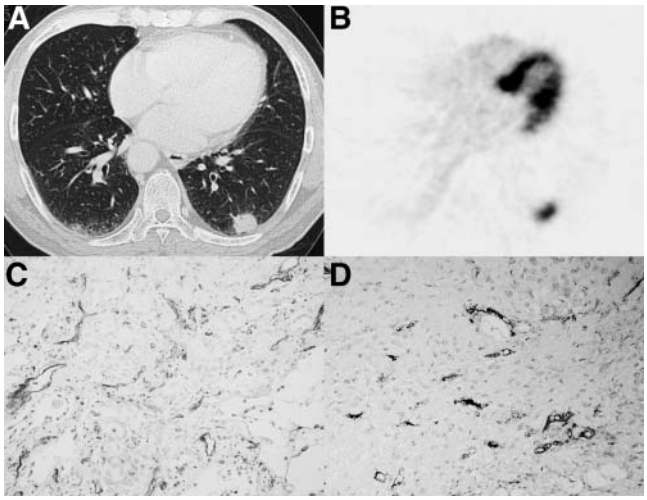

FIGURE 5. Moderately differentiated adenocarcinoma (2.9 cm) with recurrence in 23 mo. (A) CT scan shows nodule in left lung. (B) ^{18}F-FDG PET shows intense uptake of ^{18}F-FDG in tumor (SUV = 5.76). (C) CD31 immunohistochemical analysis shows high MVD. (D) CD105 immunohistochemical analysis also shows high MVD.

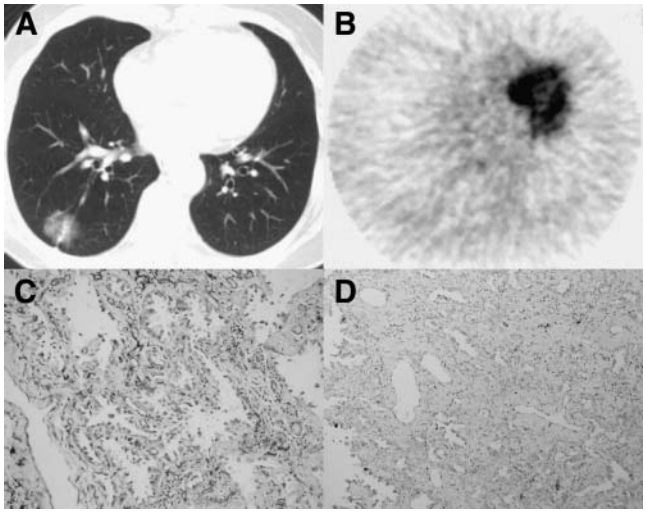

FIGURE 6. BAC (2.0 cm) without recurrence in 50 mo. (A) CT scan shows nodule in right lung. (B) ^{18}F-FDG PET shows modest uptake of ^{18}F-FDG in tumor (SUV = 1.32). (C) CD31 immunohistochemical analysis shows moderate MVD. (D) CD105 immunohistochemical analysis shows low MVD.

an urgent need for assessing pretreatment angiogenic status and evaluating the response to this therapy in clinical studies. In the present study, we found that ^{18}F-FDG uptake not only can reflect the angiogenic status in lung adenocarcinomas but also, and more importantly, can reflect active angiogenesis in lung adenocarcinomas. These properties may have further applications in assessing and monitoring antiangiogenic therapy in the near future.

CONCLUSION

In contrast to CD31-MVD, CD105-MVD reflects active tumor angiogenesis and is a better indicator of prognosis in patients with lung adenocarcinomas. ^{18}F-FDG uptake correlated significantly with the active angiogenesis determined by CD105-MVD. This property may have applications in assessing and monitoring antiangiogenic therapy.

ACKNOWLEDGMENTS

This work was supported by a Grant of Collaborative Research from Kanazawa Medical University (C2005-2), by a Grant-in-Aid for Cancer Research (16-5) from the Ministry of Health and Welfare, Japan, and by Grants-in-Aid (16591232 and 17590320) for Scientific Research from the Ministry of Education, Japan.

REFERENCES

1. Kurokawa T, Matsuno Y, Noguchi M, Mizuno S, Shimosato Y. Surgically curable "early" adenocarcinoma in the periphery of the lung. *Am J Surg Pathol.* 1994;18:431–438.
2. Takise A, Kodama T, Shimosato Y, Watanabe S, Suemasu K. Histopathologic prognostic factors in adenocarcinomas of the peripheral lung less than 2 cm in diameter. *Cancer.* 1988;61:2083–2088.
3. Charloux A, Quoix E, Wolkove N, Small D, Pauli G, Kreisman H. The increasing incidence of lung adenocarcinoma: reality or artefact? A review of the epidemiology of lung adenocarcinoma. *Int J Epidemiol.* 1997;26:14–23.
4. Hanahan D, Folkman J. Patterns and emerging mechanisms of the angiogenic switch during tumorigenesis. *Cell.* 1996;86:353–364.
5. Weidner N. Tumoural vascularity as a prognostic factor in cancer patients: the evidence continues to grow. *J Pathol.* 1998;184:119–122.
6. Giatromanolaki A, Koukourakis MI, Theodossiou D, et al. Comparative evaluation of angiogenesis assessment with anti-factor-VIII and anti-CD31 immunostaining in non-small cell lung cancer. *Clin Cancer Res.* 1997;3:2485–2492.
7. Fontanini G, Lucchi M, Vignati S, et al. Angiogenesis as a prognostic indicator of survival in non-small-cell lung carcinoma: a prospective study. *J Natl Cancer Inst.* 1997;89:881–886.
8. Pastorino U, Andreola S, Tagliabue E, et al. Immunocytochemical markers in stage I lung cancer: relevance to prognosis. *J Clin Oncol.* 1997;15:2858–2865.
9. Chandrachud LM, Pendleton N, Chisholm DM, Horan MA, Schor AM. Relationship between vascularity, age and survival in non-small-cell lung cancer. *Br J Cancer.* 1997;76:1367–1375.
10. O'Byrne KJ, Koukourakis MI, Giatromanolaki A, et al. Vascular endothelial growth factor, platelet-derived endothelial cell growth factor and angiogenesis in non-small-cell lung cancer. *Br J Cancer.* 2000;82:1427–1432.
11. Liao M, Wang H, Lin Z, Feng J, Zhu D. Vascular endothelial growth factor and other biological predictors related to the postoperative survival rate on non-small cell lung cancer. *Lung Cancer.* 2001;33:125–132.
12. Cox G, Jones JL, Andi A, Waller DA, O'Byrne KJ. A biological staging model for operable non-small cell lung cancer. *Thorax.* 2001;56:561–566.
13. Miller TR, Pinkus E, Dehdashti F, Grigsby PW. Improved prognostic value of ^{18}F-FDG PET using a simple visual analysis of tumor characteristics in patients with cervical cancer. *J Nucl Med.* 2003;44:192–197.
14. Franzius C, Bielack S, Flege S, Sciuk J, Jurgens H, Schober O. Prognostic significance of ^{18}F-FDG and ^{99m}Tc-methylene diphosphonate uptake in primary osteosarcoma. *J Nucl Med.* 2002;43:1012–1017.
15. Pandit N, Gonen M, Krug L, Larson SM. Prognostic value of [^{18}F]FDG-PET imaging in small cell lung cancer. *Eur J Nucl Med Mol Imaging.* 2003;30:78–84.
16. Higashi K, Ueda Y, Arisaka Y, et al. ^{18}F-FDG uptake as a biologic prognostic factor for recurrence in patients with surgically resected non–small cell lung cancer. *J Nucl Med.* 2002;43:39–45.
17. Hicks RJ, Kalff V, MacManus MP, et al. ^{18}F-FDG PET provides high-impact and powerful prognostic stratification in staging newly diagnosed non–small cell lung cancer. *J Nucl Med.* 2001;42:1596–1604.
18. Dhital K, Saunders CA, Seed PT, O'Doherty MJ, Dussek J. [(18)F]Fluorodeoxyglucose positron emission tomography and its prognostic value in lung cancer. *Eur J Cardiothorac Surg.* 2000;18:425–428.
19. Guo J, Higashi K, Yokota H, et al. In vitro proton magnetic resonance spectroscopic lactate and choline measurements, ^{18}F-FDG uptake, and prognosis in patients with lung adenocarcinoma. *J Nucl Med.* 2004;45:1334–1339.
20. Zasadny KR, Tatsumi M, Wahl RL. FDG metabolism and uptake versus blood flow in women with untreated primary breast cancers. *Eur J Nucl Med Mol Imaging.* 2003;30:274–280.
21. Tanaka F, Otake Y, Yanagihara K, et al. Evaluation of angiogenesis in non-small cell lung cancer: comparison between anti-CD34 antibody and anti-CD105 antibody. *Clin Cancer Res.* 2001;7:3410–3415.
22. Eberhard A, Kahlert S, Goede V, Hemmerlein B, Plate KH, Augustin HG. Heterogeneity of angiogenesis and blood vessel maturation in human tumors: implications for antiangiogenic tumor therapies. *Cancer Res.* 2000;60:1388–1393.
23. King TW, Brey EM, Youssef AA, Johnston C, Patrick CW Jr. Quantification of vascular density using a semiautomated technique for immunostained specimens. *Anal Quant Cytol Histol.* 2002;24:39–48.
24. Lee JS, Jung JJ, Kim J. Quantification of angiogenesis by a computerized image analysis system in renal cell carcinoma. *Anal Quant Cytol Histol.* 2000;22:469–474.
25. Weidner N, Semple JP, Welch WR, Folkman J. Tumor angiogenesis and metastasis: correlation in invasive breast carcinoma. *N Engl J Med.* 1991;324:1–8.
26. Vermeulen PB, Gasparini G, Fox SB, et al. Quantification of angiogenesis in solid human tumours: an international consensus on the methodology and criteria of evaluation. *Eur J Cancer.* 1996;32A:2474–2484.
27. Vermeulen PB, Gasparini G, Fox SB, et al. Second international consensus on the methodology and criteria of evaluation of angiogenesis quantification in solid human tumours. *Eur J Cancer.* 2002;38:1564–1579.
28. Risau W. Differentiation of endothelium. *FASEB J.* 1995;9:926–933.
29. Hobson B, Denekamp J. Endothelial proliferation in tumours and normal tissues: continuous labelling studies. *Br J Cancer.* 1984;49:405–413.
30. Kumar P, Wang JM, Bernabeu C. CD 105 and angiogenesis. *J Pathol.* 1996;178:363–366.
31. Burrows FJ, Derbyshire EJ, Tazzari PL, et al. Up-regulation of endoglin on vascular endothelial cells in human solid tumors: implications for diagnosis and therapy. *Clin Cancer Res.* 1995;1:1623–1634.
32. Miller DW, Graulich W, Karges B, et al. Elevated expression of endoglin, a component of the TGF-beta-receptor complex, correlates with proliferation of tumor endothelial cells. *Int J Cancer.* 1999;81:568–572.
33. Wang JM, Kumar S, Pye D, Haboubi N, al Nakib L. Breast carcinoma: comparative study of tumor vasculature using two endothelial cell markers. *J Natl Cancer Inst.* 1994;86:386–388.
34. Kumar S, Ghellal A, Li C, et al. Breast carcinoma: vascular density determined using CD105 antibody correlates with tumor prognosis. *Cancer Res.* 1999;59:856–861.
35. Wikstrom P, Lissbrant IF, Stattin P, Egevad L, Bergh A. Endoglin (CD105) is expressed on immature blood vessels and is a marker for survival in prostate cancer. *Prostate.* 2002;51:268–275.
36. Higashi K, Ueda Y, Seki H, et al. Fluorine-18-FDG PET imaging is negative in bronchioloalveolar lung carcinoma. *J Nucl Med.* 1998;39:1016–1020.
37. Tateishi U, Nishihara H, Tsukamoto E, Morikawa T, Tamaki N, Miyasaka K. Lung tumors evaluated with FDG-PET and dynamic CT: the relationship between vascular density and glucose metabolism. *J Comput Assist Tomogr.* 2002;26:185–190.
38. Yang JC, Haworth L, Sherry RM, et al. A randomized trial of bevacizumab, an anti-vascular endothelial growth factor antibody, for metastatic renal cancer. *N Engl J Med.* 2003;349:427–434.

JNM The Journal of NUCLEAR MEDICINE

Microvessel Density: Correlation with ^{18}F-FDG Uptake and Prognostic Impact in Lung Adenocarcinomas

JianFei Guo, Kotaro Higashi, Yoshimichi Ueda, Manabu Oguchi, Tsutomu Takegami, Hirohisa Toga, Tsutomu Sakuma, Hajime Yokota, Shogo Katsuda, Hisao Tonami and Itaru Yamamoto

J Nucl Med. 2006;47:419-425.

The Journal of Nuclear Medicine is published monthly.
SNMMI | Society of Nuclear Medicine and Molecular Imaging
1850 Samuel Morse Drive, Reston, VA 20190.
(Print ISSN: 0161-5505, Online ISSN: 2159-662X)

SNMMI SOCIETY OF NUCLEAR MEDICINE AND MOLECULAR IMAGING